

Ultraviolet-visible absorption of small silver clusters in neon: Ag_n ($n = 1-9$)

S. Lecoultre, A. Rydlo, J. Buttet, C. Félix,^{a)} S. Gilb,^{b)} and W. Harbich^{c)}

*Institut de Physique de la Matière Condensée, École Polytechnique Fédérale de Lausanne,
1015 Lausanne, Switzerland*

(Received 18 March 2009; accepted 13 April 2011; published online 11 May 2011)

We present optical absorption and fluorescence spectra in the UV-visible range of size selected neutral Ag_n clusters ($n = 1-9$) in solid neon. Rich and detailed optical spectra are found with linewidths as small as 50 meV. These spectra are compared to time dependent density functional theory implemented in the TURBOMOLE package. Excellent agreement between theory and experiment is achieved in particular for the dominant spectroscopic features at photon energies below 4.5 eV. This allows a clear attribution of the observed electronic transitions to specific isomers. Optical transitions associated to the s -electrons are concentrated in the energy range between 3 and 4 eV and well separated from transitions of the d -electrons. This is in contrast to the other coinage metals (Au and Cu) which show a strong coupling of the d -electrons. © 2011 American Institute of Physics. [doi:10.1063/1.3589357]

I. INTRODUCTION

The determination of the electronic structure of clusters, in particular metal clusters, is still in the focus of active research. The combination of experimental data and high level *ab initio* methods gives invaluable insight in the evolution of the electronic structure as a function of size. Several theoretical and experimental studies have been carried out on the structural and electronic properties of small silver clusters. In particular the optical response of neutral silver clusters embedded in rare gas matrices has been the object of numerous studies.^{1,2} The development of cluster sources coupled to molecular beam techniques allowed to produce beams of cations with a well defined size. After deceleration the size selected cluster cations were deposited on a sample holder at low temperature together with a rare gas and neutralized to form a seeded rare gas matrix of neutral species. Using this technique Fedrigo *et al.*³⁻⁵ measured the optical absorption of silver neutral clusters at low temperature embedded in rare gas matrices (Ar, Kr, Xe). It was however not possible to measure the absorption spectra of Ag_4 , Ag_6 , Ag_{10} , Ag_{12} , Ag_{14} clusters due to their low abundance in the molecular beam. More recently a new absorption setup was developed⁶ by elongating the optical path and thus increasing the sensitivity. This allowed to measure, in an argon matrix grown at 28 K, the absorption spectra of all clusters up to Ag_{14} .⁷

On the theoretical side several studies within different approximations have calculated the equilibrium geometries and electronic properties of silver clusters taking explicitly into account the effect of the d electrons. The absorption spectra of Ag_n ($n = 2-8$) in the UV-Visible range have been determined in the framework of the linear response

equation-of-motion coupled cluster method⁸⁻¹⁰ and more recently within the time dependent density functional theory (TD-DFT) approximation^{7,11-16} for clusters containing up to 120 atoms. The reasonably good agreement between the main features of the experimental and theoretical data allowed to assign the measured spectra to given isomers,^{7,12} however several differences are still present. In order to test the validity of different theoretical approximations, it is crucial to compare the calculated spectra with the measured one's down to the smallest available details. The ideal case, gas phase absorption spectra at cryogenic temperatures are experimentally not accessible. Neon provides a weakly interacting medium, revealing numerous details as shown for selected sizes in Ag_n/Ne ,¹⁷ Cu_n/Ne ,¹⁸ and Au_n/Ne .¹⁹ We present here a new series of absorption measurements on silver clusters (Ag_n ($n = 1-9$)) deposited at 6 K in solid neon. The main features of these new data are similar to those obtained in other rare gas matrices,^{4,5,7} however spectra show much better resolution and structures not present in previous measurements are clearly seen. We suggest that these measurements shall be taken as a benchmark for actual and future calculations on neutral silver clusters.

II. EXPERIMENTAL AND COMPUTATION

The experimental setup and measurement procedure are described in Ref. 6. Briefly, the clusters are formed from a metal target sputtered by a 10 mA Xe^+ ion beam at 25 keV. The cations are then focused into a "Bessel Box" type (BB) energy filter which also acts as a beam stop for the intense flux of neutrals. The cations of interest are mass-selected and directed towards the sample holder, which consists in a superpolished aluminium mirror (Valley Design Corp.). The sample holder is fixed to a cold head cryostat (SRP-052A Cryocooler, Sumitomo Heavy Industries Ltd.) that allows refrigeration to about 6 K. During sample preparation, the size-selected clusters are accumulated together with a 50 μm neon matrix.

^{a)}Present address: Meteo Swiss, 1530 Payerne, Switzerland.

^{b)}MS-ROK Research Informatics, Merck KGaA, Frankfurter Str. 250 64293 Darmstadt, Germany.

^{c)}Electronic mail: wolfgang.harbich@epfl.ch.

Optical absorption measurements are performed by injecting light through the 2 mm length of the matrix and collecting the residual light on the other side with a solarization resistant optical fiber of 400 μm core diameter. The collected light is analyzed by an optical spectrometer coupled to a liquid-nitrogen-cooled charge coupled device. Comparing the intensity of the light passing through a matrix doped with clusters to a reference signal of light passing through a pure neon matrix yields the absorption spectrum. For silver clusters, deposition times had to be adjusted between 30 to 90 min depending on the cluster size. For each spectrum presented here, the absorption rate is comprised between 70% and 95%. Special care has been taken in order to avoid saturation effects of the strongest absorption peaks.

For the TD-DFT calculation of the optical spectra, a computational scheme was used which is also suitable for the other coinage metals. The b3-lyp (Refs.20 and 21) functional together with the def2-TZVP basis ((7s7p6d1f)/[6s4p3d1f]) as implemented in the TURBOMOLE package was chosen.²² The inner 28 electrons were described using the respective effective core potential. Quadrature grids were of m3 quality.²³ The geometry optimization was started using structures found in the literature and at least the two lowest lying isomers from Ref. 24 were evaluated. The geometry optimizations are carried out with symmetry restriction where applicable. In all cases the force matrix was calculated to ensure local minima in contrast to saddle points. Complete consistency has been found by comparing the lowest energy structures with previous results,^{7,9-16,24} except for Ag_3 . In this case the b3-lyp functional fails to describe the geometry. Based on high level calculations and on the experimental results we have chosen an opening angle of 67°, well in the expected range of density functional theory.

The TD-DFT calculations were performed with the ESCF module²⁵ of the TURBOMOLE V-5.9 program package.²⁶ Up to the pentamer, dipole allowed and non-allowed transitions were calculated up to an excitation energy of 7 eV. For Ag_n , $n=(6-9)$ all dipole allowed transitions up to 7 eV were evaluated.

III. RESULTS AND DISCUSSION

The lower trace of Fig. 1 (red curve) presents size by size the measured absorption spectra of Ag_n , $n=1-9$ for clusters embedded in a neon matrix at 7 K. The upper trace (black curve) corresponds to the present TD-DFT calculation for the best fitting isomer, and in the case of Ag_6 , Ag_8 , and Ag_9 to the two lowest energy isomers.

Table I gives the peak position and oscillator strength of the different transitions observed experimentally. They have been obtained by deconvoluting the measured spectra in a sum of Gaussians. Their position was chosen in order to correspond to the measured peak position, while their linewidth and amplitude were determined by a least square fit. The integrated cross section for a given transition was determined by integrating the corresponding line shape, its absolute value depends then on the cluster density.

TABLE I. Peak position in eV and in parenthesis integral of the cross-section over the energy of the corresponding transition. The oscillator strength is obtained by multiplying the integrated cross section (in $10^{-18} \text{ cm}^2 \text{ eV}$) by 1.12×10^{-2} .

Species	Peak position (oscillator strength) [eV] ($[\text{cm}^2] \times 10^{-18}$)
Ag_1	3.80(3.83), 3.87(10.7) , 4.00(25.0) , 4.12(10.4) , 4.20(12.2)
Ag_2	2.96(32.1) , 4.68(18.1) , 4.78(14.5) , 4.85(12.2) , 5.07(11.8)
Ag_3	2.46(0.82), 2.53(7.06), 2.75(2.75), 3.07(12.4) , 3.24(2.62), 3.51(16.7) , 3.71(29.5) , 3.87(5.02), 3.99(12.7) , 4.12(6.3), 4.48(4.71), 4.66(0.32), 4.78(3.14), 5.01(6.38), 5.17(6.73), 5.44(4.87), 3.07(29.9) , 4.23(18.7) , 4.48(2.83), 4.66(5.60), 5.08(4.79), 5.34(1.37), 5.43(5.75)
Ag_4	2.00(5.48), 2.57(3.37), 3.11(2.81), 3.27(45.0) , 3.56(7.02), 3.69(28.1) , 3.81(12.5), 4.11(4.64), 4.44(3.37), 4.60(4.07), 4.85(3.37), 4.95(2.95), 5.36(15.9), 5.62(6.46)
Ag_5	2.86(11.9), 3.10(10.7), 3.45(74.8) , 3.53(17.6), 3.65(34.0) , 3.89(3.20), 4.00(14.3), 4.87(14.2), 5.01(13.6), 5.25(26.4), 5.59(26.2)
Ag_6	2.78(6.28), 3.43(6.82), 3.64(103) , 3.79(28.2), 3.95(1.73), 4.07(13.3), 4.48(13.4), 4.63(26.9), 4.86(17.4), 5.38(12.9)
Ag_7	2.55(1.55), 3.12(12.1), 3.20(11.4), 3.65(38.0), 4.00(139) , 5.40(20.7)
Ag_8	2.26(3.64), 2.51(2.58), 2.79(1.83), 3.05(8.22), 3.26(0.43), 3.47(21.8), 3.65(27.7), 3.73(26.3), 3.84(87.7) , 3.98(13.9), 4.14(107) , 4.24(2.22), 4.49(9.26)
Ag_9	2.26(3.64), 2.51(2.58), 2.79(1.83), 3.05(8.22), 3.26(0.43), 3.47(21.8), 3.65(27.7), 3.73(26.3), 3.84(87.7) , 3.98(13.9), 4.14(107) , 4.24(2.22), 4.49(9.26)

A. Comparison to previous experimental results

As can be seen at a first glance in comparing Fig. 1 and the experimental spectra reported in Harb's paper,⁷ the present spectra are much better resolved. Although the overall absorption spectrum looks similar, small structures not visible previously clearly appear.

Ag_1 The experimental spectrum of Ag_1 in neon is composed of four distinct peaks and a shoulder at 3.80 eV. The negative peak at 3.75 eV is due to the $^2D_{5/2} \rightarrow ^2S_{1/2}$ emission that is captured by the optical fiber. It is in good agreement with previous measurements.^{27,28} The multiplicity of lines has been explained by the spin-orbit coupling which lifts the degeneracy of the $S \rightarrow P$ transition, the effect of the crystal field splitting, and the presence of two sites of 3 and 4 neon vacancies.²⁹ This multiplicity of site isomers is not observed in argon, nor in other matrices.^{3,4}

Ag_2 The experimental spectrum of Ag_2 in neon consists of four narrow peaks at 2.96, 4.68, 4.78, and 5.07 eV and an additional transition at 4.85 eV that appears as a shoulder. The small structures between 3.75 and 4.2 eV result from fragmentation and correspond to the Ag atomic absorption lines. The negative peak at 3.56 eV is due to the fluorescence of the dimer. The silver dimer has been extensively studied in matrices,³⁰ as well as in the gas phase.^{31,32} In particular absorption in neon was already obtained by Schrittenlacher *et al.*

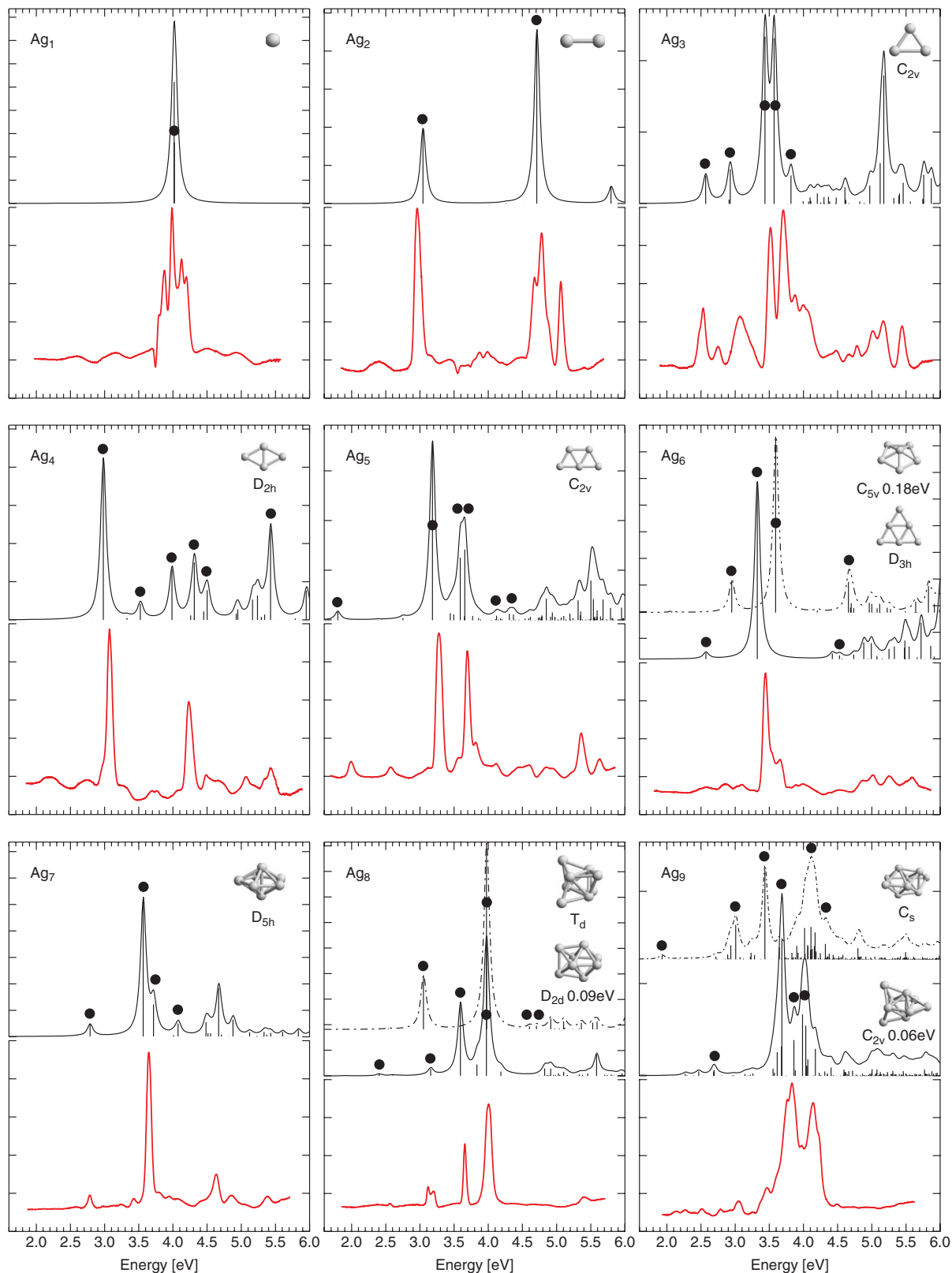


FIG. 1. Comparison between experimental and calculated absorption spectra of silver clusters. Experimental absorption for Ag_n ($n = 1-9$) – bottom curve. TD-DFT calculations for the best fitting isomer – continuous line – and energetically closest isomer – interrupted line. The energy in eV represents the difference to the calculated ground state configuration. The transitions have been enlarged by Lorentzians of 0.1 eV FWHM. The vertical scale for the calculated spectra is a measure of the oscillator strength per atom, one interval corresponding to 0.1 units for Ag_1 and Ag_2 , 0.05 units for Ag_3 to Ag_9 . The black dots identify transitions whose initial state is predominantly of s -type.

between 2 and 10 eV.³³ The measured absorption peaks at 3.00, 4.68, 4.79, and 5.08 eV are in excellent agreement with our results. They were assigned to the so-called A, B, C, and E transitions measured in the gas phase.^{34,35} The shoulder at 4.85 eV, not observed previously, can be related to the D transition observed in the gas phase at 4.84 eV.

Ag₃ Contrary to the case of Ag₃ in an argon matrix grown at 10 K^{5,36,37} which shows essentially three resolved absorption lines at 2.52, 3.21, and 3.86 eV, the Ag₃/Ne spectrum is formed of a large number of narrow transitions, including two major peaks at 3.51 and 3.71 eV, that we all attribute to the trimer absorption, since there is no sign of fragmentation during deposition. Existing measurements of the trimer in helium droplets by Federmann *et al.*³⁸ reveal distinct peaks in good agreement with the two major peaks if we consider a blueshift of 0.07 eV in neon compared to helium. The large difference between the neon and argon matrix absorption spectra is surprising. We believe that the equilibrium geometry of Ag₃, which has a flat potential curve, depends on its interaction with the matrix.

Ag₄ A very good signal to noise ratio is difficult to obtain in the case of Ag₄, since the abundance of the tetramer cation in the mass spectrum is low. We find that the absorption spectrum of Ag₄ is composed of two main transitions at 3.07 and 4.23 eV, as well as smaller intensity transitions (see Table I). The other lines present in the spectrum should be considered as artefacts for the reason given above.

The two lowest energy transitions correspond well to the main peaks observed in argon at 3.07 eV and 4.15 eV.^{7,39} We find in argon an intense peak at 4.50 eV, which is not present or barely visible in neon. It was suggested⁷ that it corresponds to symmetry forbidden transitions lifted by the interaction with the matrix. Its absence in the weakly perturbing neon matrix supports this idea.

Ag₅ Two major transitions at 3.27 and 3.69 eV are observed, as well as many lower intensity transitions. The spectrum obtained in neon looks similar to that in argon, but with narrower and better resolved peaks as well as more details in the fine structure. It is interesting to notice that the 3.27 eV peak is barely shifted to the blue, while the 3.69 eV is shifted to the red, compared to argon, by 0.1 eV. This is an indication that the simple picture taking only into account the dielectric constant of the matrix, which would predict an average shift to the blue, must be refined for small aggregates.

Ag₆ The measured spectrum of Ag₆ shows mainly one intense and narrow transition at 3.45 eV with a shoulder at 3.65 eV. The measurements in argon⁷ showed two distinct double peaks at an average value of 3.63 and 4.15 eV, the latter structure being not visible in neon.

Similarly to the case of Ag₄ it was suggested⁷ that the double structure at 4.15 eV in argon is related to symmetry forbidden transitions lifted by matrix interaction. Its absence in the neon spectrum supports this hypothesis.

Ag₇ The spectrum of Ag₇ in neon is mainly formed of a main peak at 3.64 eV with a weak shoulder on the high energy side, and well defined smaller amplitude peaks. The peaks at 3.64 and 4.63 eV are also present in argon, krypton, and xenon matrices, as well as the shoulder on the high energy side of the

main peak, if we take into account an increasing shift to the blue from Xe to Ne.⁴

Ag₈ Ag₈ in neon has a well defined spectrum, with intense and narrow peaks at 3.12–3.20, 3.65, and 4.00 eV, and smaller structures at 2.55 and 5.40 eV. It is in excellent agreement with the measured spectrum in an argon matrix, whose corresponding peaks are situated at 3.15, 3.57, and 3.82–3.90 eV. R2PI measurements of Ag₈ in He droplets^{38,40} have also been performed, they reveal a narrow structure centered at 3.96 eV and a shoulder at 3.99 eV corresponding clearly to the main absorption peak observed in neon and argon (FWHM equal to 56 meV, 0.1 eV, 0.2 eV in He, Ne, Ar).^{7,41}

Ag₉ In the case of Ag₉ in an argon matrix⁴² the shape of the spectrum could only be explained by assuming that several isomers coexisted in the matrix. The absorption spectrum in neon is clearly different.

The analysis suggests that, contrary to the case of argon, one predominant cluster geometry is present in a neon matrix.

B. Matrix effects in silver clusters

Compared to the other matrices,^{4,5,7} except helium,^{38,40} the measurements in neon show narrower structures and an improved resolution because of the weaker cluster support interaction. Comparison between the argon and neon results shows that the purely dielectric effect⁴ has to be refined. Gervais *et al.*^{43,44} showed that the effect of the matrix is the result of two competing effects, the Pauli repulsion on one side and the long range polarization of the matrix on the other side. These competing effects may lead to a shift depending, for a given isomer, on the observed transition. This was clearly the case (see above) for Ag₅ and Ag₈, while the dielectric effect alone explains well the shifts measured, e.g., for Ag₇.⁵ The effect of the matrix induces small changes in the geometrical structure of embedding clusters, which may have a large influence on the oscillator strength of the different transitions.^{10,43,44} Also symmetry forbidden transitions may be lifted by interaction with the matrix, we suggest that this is the case for Ag₄ and Ag₆ clusters in an argon matrix. The delocalized nature of the conduction electrons leads to isomers of close ground state energies. In silver this is the case for Ag₃, Ag₆, Ag₈, and Ag₉. We thus expect that different isomers are present in the matrix. Furthermore, the cluster stabilization energy differs from one matrix to the other^{43,44} suggesting that the relative weight of different isomers depends on the embedding matrix. A detailed analysis indicates that these effects are present in the case of Ag₆, Ag₈, and Ag₉ clusters. We expect that, when the number of atoms per cluster increases, the occurrence of several isomers in the matrix will be the standard situation. This sets a limit to the determination of the geometrical structure of metallic clusters in a matrix, except for very symmetric geometries.

C. Comparison to TD-DFT calculations

Several calculations of the absorption spectra of silver clusters are available in the literature, we refer the reader to

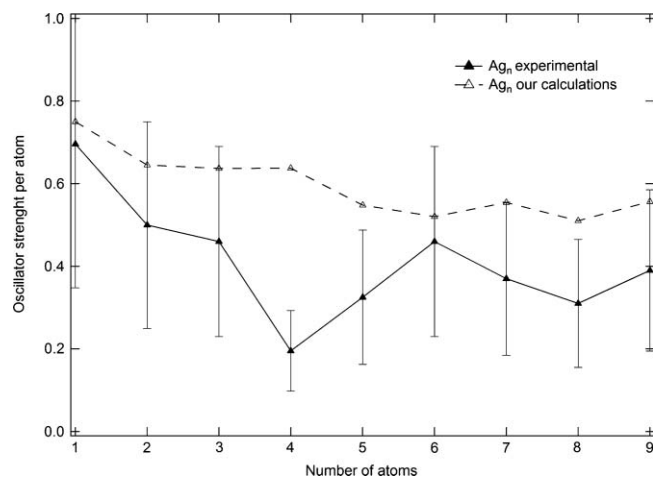


FIG. 2. Experimental and theoretical values of the oscillator strength per atom for Ag_n ($n=1-9$) clusters integrated up to a photon energy of 5.5 eV. The theoretical value has been reported for the ground state configuration. The systematic error of 50% on the measured absolute value is related to the uncertainty in determining the density of clusters per unit area.

the paper of Harb *et al.*⁷ for a comparison between different approximations and to the recent paper by Tiago *et al.*¹⁶ The TD-DFT absorption spectra reported in Fig. 1 are in agreement with the main features of previous calculations done in the same formalism,^{7,12,13} and differ in details or in the relative amplitude of the different absorption peaks. They are given here (see Fig. 1) for convenience and later on in order to compare within the same approximation the absorption spectra of Ag, Au,¹⁹ and Cu (Ref. 18) clusters. Harb *et al.* made already a detailed comparison of the experimental absorption spectra of Ag cluster in an argon matrix with their TD-DFT calculations. The good agreement between the main features of the experimental and theoretical data allowed to assign the measured spectra to given isomers or to a sum of isomers. An analysis based on the present TD-DFT calculation and the new neon results reaches the same conclusions, we shall not repeat it. Notice however that the agreement between experiment and theory is based on the principal absorption peaks of energy lower than 4.5 eV. For higher energies and smaller amplitude structures, the correlation between experiment and theory becomes poor. A Mulliken population analysis of the states implied in the different transitions indicates that the transitions below 4.5 eV are issued from predominantly *s* type states (marked by a black dot in Fig. 1), while above 4.5 eV they are issued from *d* type states. This suggests that the TD-DFT scheme does not reproduce well the transitions issued from *d* type states, and/or that the matrix effects and spin-orbit coupling have to be taken into account in order to reproduce the fine details of the absorption spectra. Notice also that the present TD-DFT calculation for the rhombus Ag_4 isomer shows significant differences with the experimental results in the 3.5–4.5 eV energy range. On the contrary the elaborate CI calculations by Koutecký *et al.*^{8,9} lead to excellent correspondence for the two main experimental peaks calculated at 3.21 eV (expt. 3.07 eV) and 4.29 eV (expt. 4.23 eV).

D. Oscillator strength

Figure 2 presents the experimental and theoretical values of the sum of the oscillator strength (OS) per atom for the Ag_n ($n=1-9$) clusters up to a cutoff energy of 5.5 eV. For the atom the measured value of the OS, equal to 0.70, is in good agreement with the gas phase value⁴⁵ equal to 0.71. This is not the case for Au_1 and Cu_1 for which the gas phase value is significantly larger (factors equal to 3.7 and 2.5 for Au and Cu, respectively) than the OS in the neon matrix. It has been suggested⁴⁶ that in the case of Cu and Au the screening of the *s* electrons is modified by the presence of the matrix, this is clearly not the case for the Ag atom. Both experiment and theory find the integrated OS per atom (or *s* electron) to be lower than one. As already mentioned by Idrobo *et al.*^{12,13} the reason for this is the screening of the electromagnetic field acting on the *s* electrons by the polarizability of the *d* electrons. A more refined analysis should also take into account the contribution of the *d-s* and *d-p* transitions to the OS. We find in agreement with Idrobo's calculation that the degree of *d* character of the optical excitations is smaller than 20% up to an excitation energy of 5.5 eV. In the case of Au (Ref. 19) and Cu (Ref. 18) clusters, the absolute value of the measured OS is definitely smaller than for Ag clusters. This can be related to the increased screening of the *s* electrons in going from Ag, to Cu and Au, and possibly to the effect of the matrix.

IV. CONCLUSION

We present optical absorption spectra of mass selected Ag_n ($n=1-9$) clusters in the UV-visible range embedded in a solid neon matrix. The main features of these new data are similar to those obtained in an argon or xenon matrix. However the improved resolution and the small interaction of the clusters with the neon matrix reveal new structures. In agreement with previous analyses we find that the main spectroscopic features are well reproduced by TD-DFT calculations for energies lower than 4.5 eV. This allows to confirm the geometrical structures of the isomers present in the matrix. However several detailed features of the measured spectra are not explained by TD-DFT calculations, in particular above 4.5 eV where the *d* electrons contribution to the transitions is important. We suggest that it is on one hand due to the influence of the matrix, which is not taken into account in the present theoretical approaches, and on the other hand on the approximations of the theories themselves. In order to discriminate between different approximations detailed experimental results are requested, the present measurements can serve as benchmark to test the validity of different theoretical approaches.

ACKNOWLEDGMENTS

This work has been supported by the Swiss National Science Foundation [NSF(CH)].

¹G. A. Ozin and H. Hubert, *Inorg. Chem.* **17**, 155 (1978).

²D. M. Gruen and J. K. Bates, *Inorg. Chem.* **16**, 2450 (1977).

- ³W. Harbich, S. Fedrigo, F. Meyer, D. M. Lindsay, J. Lignieres, J. C. Rivoal, and D. Kreisle, *J. Chem. Phys.* **93**, 8535 (1990).
- ⁴S. Fedrigo, W. Harbich, and J. Buttet, *Int. J. Mod. Phys. B* **6**, 3767 (1992).
- ⁵S. Fedrigo, W. Harbich, and J. Buttet, *Phys. Rev. B* **47**, 10706 (1993).
- ⁶F. Conus, J. T. Lau, V. Rodrigues, and C. Félix, *Rev. Sci. Instrum.* **77**, 113103 (2006).
- ⁷M. Harb, F. Rabilloud, D. Simon, A. Rydlo, S. Lecoultre, F. Conus, V. Rodrigues, and C. Félix, *J. Chem. Phys.* **129**, 194108 (2008).
- ⁸V. Bonačić-Koutecký, M. Boiron, J. Pittner, P. Fantucci, and J. Koutecký, *Eur. Phys. J. D* **9**, 183 (1999).
- ⁹V. Bonačić-Koutecký, J. Pittner, M. Boiron, and P. Fantucci, *J. Chem. Phys.* **110**, 3876 (1999).
- ¹⁰V. Bonačić-Koutecký, V. Veyret, and R. Mitrić, *J. Chem. Phys.* **115**, 10450 (2001).
- ¹¹K. Yabana and G. F. Bertsch, *Phys. Rev. A* **60**, 3809 (1999).
- ¹²J. C. Idrobo, S. Ögüt, and J. Jellinek, *Phys. Rev. B* **72**, 085445 (2005).
- ¹³J. C. Idrobo, S. Ogut, K. Nemeth, J. Jellinek, and R. Ferrando, *Phys. Rev. B* **75**, 233411 (2007).
- ¹⁴L. Jensen, L. L. Zhao, and G. C. Schatz, *J. Phys. Chem. C* **111**, 4756 (2007).
- ¹⁵C. M. Aikens, S. Li, and G. C. Schatz, *J. Phys. Chem. C* **112**, 11272 (2008).
- ¹⁶M. Tiago, J. Idrobo, S. Ogut, J. Jellinek, and J. Chelikowsky, *Phys. Rev. B* **79**, 155419 (2009).
- ¹⁷W. Harbich, Y. Belyaev, R. Kleiber, and J. Buttet, *Surf. Rev. Lett.* **3**, 1147 (1996).
- ¹⁸S. Lecoultre, A. Rydlo, J. Buttet, C. Félix, S. Gilb, and W. Harbich, *J. Chem. Phys.* **134**, 074303 (2011).
- ¹⁹S. Lecoultre, A. Rydlo, J. Buttet, C. Félix, S. Gilb, and W. Harbich, *J. Chem. Phys.* **134**, 074302 (2011).
- ²⁰A. Becke, *Phys. Rev. A* **38**, 3098 (1988).
- ²¹C. Lee, W. Yang, and R. Parr, *Phys. Rev. B* **37**, 785 (1988).
- ²²F. Weigend and R. Ahlrichs, *Phys. Chem. Chem. Phys.* **7**, 3297 (2005).
- ²³O. Treutler and R. Ahlrichs, *J. Chem. Phys.* **102**, 346 (1995).
- ²⁴E. M. Fernández, J. M. Soler, I. L. Garzón, and L. C. Balbás, *Phys. Rev. B* **70**, 165403 (2004).
- ²⁵R. Bauernschmitt and R. Ahlrichs, *Chem. Phys. Lett.* **256**, 454 (1996).
- ²⁶R. Ahlrichs, M. Bar, H. H. M. Haser, and C. Kolmel, *Chem. Phys. Lett.* **162**, 165 (1989).
- ²⁷W. Schrittenlacher, H. H. Rotermund, W. Schroeder, and D. M. Kolb, *Surf. Sci.* **156**, 777 (1985).
- ²⁸J. T. Zoueu, M. Vala, and J. C. Rivoal, *Chem. Phys.* **312**, 89 (2005).
- ²⁹S. Ossicini and F. Forstmann, *Inorg. Chem.* **21**, 1755 (1982).
- ³⁰S. Fedrigo, W. Harbich, and J. Buttet, *J. Chem. Phys.* **99**, 5712 (1993).
- ³¹M. D. Morse, *Chem. Rev.* **86**, 1049 (1986).
- ³²V. Beutel, H.-G. Krämer, G. L. Bhale, M. Kuhn, K. Weyers, and W. Demtröder, *J. Chem. Phys.* **98**, 2699 (1993).
- ³³W. Schrittenlacher and D. M. Kolb, *Ber. Bunsenges. Phys. Chem.* **88**, 492 (1984).
- ³⁴B. Kleman and S. Linkvist, *Arkiv Fysik* **9**, 385 (1954).
- ³⁵C. Shin-Piaw, W. Loong-Seng, and L. Yoke-Seng, *Nature (London)* **209**, 1300 (1966).
- ³⁶S. Lecoultre, A. Rydlo, and C. Felix, *J. Chem. Phys.* **126**, 204507 (2007).
- ³⁷I. Rabin, W. Schulze, G. Ertl, C. Félix, C. Sieber, W. Harbich, and J. Buttet, *Chem. Phys. Lett.* **320**, 59 (2000).
- ³⁸F. Federmann, K. Hoffmann, N. Quaas, and J. P. Toennies, *Eur. Phys. J. D* **9**, 11 (1999).
- ³⁹C. Félix, C. Sieber, W. Harbich, J. Buttet, I. Rabin, W. Schulze, and G. Ertl, *Chem. Phys. Lett.* **313**, 105 (1999).
- ⁴⁰T. Diederich, J. Tiggesbäumker, and K. H. Meiwes-Brower, *J. Chem. Phys.* **116**, 3263 (2002).
- ⁴¹C. Félix, C. Sieber, W. Harbich, J. Buttet, I. Rabin, W. Schulze, and G. Ertl, *Phys. Rev. Lett.* **86**, 2992 (2001).
- ⁴²C. Sieber, J. Buttet, W. Harbich, C. Félix, R. Mitrić, and V. Bonačić-Koutecký, *Phys. Rev. A* **70**, 041201 (2004).
- ⁴³B. Gervais, E. Giglio, E. Jacquet, A. Ipatov, P.-G. Reinhard, F. Fehrer, and E. Suraud, *J. Chem. Phys.* **121**, 8466 (2004).
- ⁴⁴B. Gervais, E. Giglio, E. Jacquet, A. Ipatov, P.-G. Reinhard, F. Fehrer, and E. Suraud, *Phys. Rev. A* **71**, 015201 (2005).
- ⁴⁵J. E. Sansonetti and W. C. Martin, *Handbook of Basic Atomic Spectroscopic Data* (National Institute of Standards and Technology, Gaithersburg, 2005).
- ⁴⁶D. M. Gruen, S. L. Gaudioso, R. L. McBeth, and J. L. Lerner, *J. Chem. Phys.* **60**, 89 (1974).